AN ANALYSIS OF THE BANDWIDTH OSCILLATIONS CAUSED BY FINITE GROUND PLANES USING CHARACTERISTIC MODE THEORY

BY

NICOLE L BOHANNON

THESIS

Submitted in partial fulfillment of the requirements
for the degree of Master of Science in Electrical and Computer Engineering
in the Graduate College of the
University of Illinois at Urbana-Champaign, 2013

Urbana, Illinois

Adviser:

Professor Jennifer T. Bernhard

ABSTRACT

It has long been known that the impedance bandwidth for planar inverted-F antennas (PIFAs) changes as the rectangular ground plane changes length. Although previous research has characterized these changes, it has failed to adequately explain why the bandwidth and pattern changes occur. This thesis explains why these changes in bandwidth and radiation occur by creating a method for separating the effects of the ground plane from the effects of the antenna element. By replacing the element with an infinite ground plane, the structure can be analyzed including the effect of the feed and height, without including the antenna element. This structure is then analyzed using characteristic mode theory to correlate the modal behavior of the ground plane with the bandwidth minima and maxima. Overall, bandwidth minima occur for ground plane sizes where only one mode has the highest modal significance across the band, and bandwidth maxima occur when two modes shift the mode with the highest modal significance near the center frequency of the antenna.

Because the developed process is not specific to PIFAs, it is then applied directly to two different planar electrically small antennas (ESAs). The narrow bandwidth that plagues ESAs makes it particularly attractive to understand where bandwidth maxima occur to create optimal designs. At first glance the process seems to fail to predict maxima for some ground plane lengths because the ground plane size where the two modes switch is slightly larger than predicted. However, the characteristic mode simulations must be done using a perfect electric conductor (PEC), whereas the bandwidth simulations are done using copper. By investigating the effect of using copper versus PEC, the shift in center frequency is quantified. Using PEC significantly lowers the center frequency of the antenna, causing the characteristic mode model to show the transition at a larger ground plane size.

To my family, for their never ending love and support.

ACKNOWLEDGMENTS

I would like to thank Professor Jennifer Bernhard for her help, guidance, and support while completing this research.

I would also like to thank the U.S. Army Research Office for financial support through research grant W911NF-10-1-0274.

TABLE OF CONTENTS

CHAPTER 1

INTRODUCTION

1.1 Background

As technology continues to progress, electronics are continually becoming smaller, packing more functionality into smaller spaces. Restricting the size of the antenna is a tradeoff between gain, bandwidth, and efficiency. For each application these small antennas must be optimized within the volume provided. Many researchers have studied the impact of electrically small antenna (ESA) elements but often assume either a balanced dipole-like structure or an infinitely large ground plane. These assumptions are often unachievable in practical applications. Also, many times practical applications require the use of planar antennas because they achieve relatively good performance while being inexpensive and easy to manufacture. These planar antennas often have ground planes that cannot be assumed to be infinitely large. Also, the ground planes are also often irregularly shaped and because the antenna is small, the ground plane size and shape have a significant effect on antenna performance. By taking the finite size of the ground plane into account, planar antenna designs can have better performance compared to optimizing only the antenna element.

1.2 Previous Work

1.2.1 Electrically Small Antennas

Much antenna work has focused on finding physical limits for small antennas. To define an ESA, the antenna is first enclosed in a theoretical sphere with radius a, where a is the smallest possible radius where the antenna still fits

entirely in the sphere. With k defined as

$$k = \frac{2\pi}{\lambda}, \tag{1.1}$$

an ESA is defined to be an antenna where $ka < 1$. Although this work began with Wheeler in 1947, Chu furthered the theory [1]. In 1948, Chu wrote a paper detailing the equivalent circuits for small antennas and defined minimum Q and maximum gain limits for ESAs [2]. By simplifying the equations and circuits given by Chu, antenna designers found the maximum Q for a certain size of antenna. Chu's maximum Q equations simplify to

$$Q = \frac{1 + 2k^2a^2}{k^3a^3[1 + k^2a^2]}, \tag{1.2}$$

which is usually further approximated because ka is close to zero as

$$Q_{Chu} = \frac{1}{(ka)^3}. \tag{1.3}$$

Because waves in free space are expressed in spherical modes, the most efficient volume to use is a sphere. To generate spherical modes, the current is equivalent to a shell on the outside of the sphere. In his analysis Chu neglects the energy stored inside the ka sphere. Since his work neglects this point, his analysis leads to a calculation for minimum Q smaller than physically achievable.

After the work by Chu and Wheeler, many different researchers also began studying and justifying the results found by Chu and Wheeler. Collin and Rothschild also use spherical and cylindrical propagating modes to solve analytically for Q without simplifying to equivalent circuits like Chu [3]. McLean does his own derivation for a minimum Q using an ideal Hertzian dipole and the approximations for zeroth and first order spherical Bessel functions [4]. McLean finds through his calculations that

$$Q = \frac{1}{k^3a^3} + \frac{1}{ka}. \tag{1.4}$$

McLean's and Collin and Rothschild's equations for Q simplify to Chu's limit as ka gets small. Later, Thal uses equivalent circuit ladder networks much like the ones Chu described to create a new limit to account for energy

that is necessarily stored inside the ka sphere [5]. Because previous theory neglected the stored energy, the minimum Q allowed for larger bandwidth than physically achievable. Thal's research also addressed coupling between modes and the ability to use a higher order mode to maintain pattern integrity while tuning the desired mode. His work also explained why antenna designs using small singly resonant structures were struggling to reach the Chu limit. It is not physically possible using current materials.

Although theory helps to understand what is physically possible, much effort has also been put into building antennas that are close to the Thal and Chu limits for minimum Q [6]-[7]. To compare the built antennas to the proposed limits, Sievenpiper compiled a list of measured results for ESAs published in *IEEE Transactions on Antennas and Propagation* [8]. Wire cage antennas like those built by Adams et al. and Best performed closest to the theoretical limits for single and dual mode antennas [6]-[7].

Spherical antennas are an important first step in minimizing Q and maximizing bandwidth. Unfortunately antenna designers rarely have the opportunity to build spherical antennas, as they often do not fit inside traditional radiating equipment. To attempt to find minimum Q for different shapes that are more realistic, Gustaffson et al. uses scattering theory to find minimum Q for antennas with arbitrary shape [9]-[10]. These works allow antenna designers to build in shapes other than a sphere and compare to the minimum Q and bandwidth efficiency products predicted. The scattering dyadic and much of the mathematical foundation for the work by Gustafsson et al. is inaccessible to most antenna engineers. To try to correct this issue, Yaghjian and Stuart developed a method for calculating Q using the surface equivalence principle [11]. Vandenbosh also tries to make the theory more accessible by using a method that is solvable using method of moments code that many antenna designers should also be familiar with because of the application of method of moments to solving electromagnetic problems for the fields [12]. Although these methods use more familiar techniques, they are still complex theories and difficult to apply to new antenna shapes. Other than the general insight that different shapes use volume less effectively than a sphere, these references also do not offer much insight into how to design an electrically small antenna. Van Niekerk uses calculations to compare his cylindrical antennas to Gustaffson's limit for cylindrical antennas [13]. He was able to design and build ESAs close to the bandwidth efficiency product

limits for cylindrical volumes shown in [9] using a cylinder with a height to width ratio of 1:1, a capacitive feed disk and a meandered shorting pin.

1.2.2 Characteristic Mode Theory

Recently researchers have been using characteristic modes to design antennas and match ESAs. Characteristic mode theory was introduced in 1971 by Garbacz and Turpin explaining how a structure supported nonphysical modes, independent of the excitation, that could be used to estimate antenna performance [14]. Harrington and Mautz expanded on the theory of characteristic modes by demonstrating that the solution for the modes could be found using an eigenvalue problem and could be solved using the method of moments [15]. The theory uses the method of moments impedance matrix, Z, which can be decomposed into its real and imaginary parts as

$$[Z] = [R] + j[X]. \tag{1.5}$$

Harrington and Mautz derived equations relating R, X, eigenvalues (λ_n), and modal currents (J_n) that can be summarized as

$$X\left(J_n\right) = \lambda_n R\left(J_n\right). \tag{1.6}$$

Using Equation 1.6 and the impedance of the antenna, it is possible to find the modal currents and eigenvalues. The modal currents and the eigenvalues relate to the total current on the structure using Equation 1.7, where V_n^i are the modal weights and can be found using Equation 1.8, where J^i and M^i are the magnetic and electric currents that generate the incident electric and magnetic fields, respectively, and E_n and H_n are the electric and magnetic fields, respectively, resulting from modal current J_n:

$$J = \sum_n \frac{V_n^i J_n}{1 + j\lambda_n} \tag{1.7}$$

$$V_n^i = \iiint_V E_n \dot{J}^i - H_n \dot{M}^i. \tag{1.8}$$

Recently, the theory of characteristic modes was revisited and applied directly to plates and antennas in a comprehensive review [16]. The value of λ_n

indicates how well the mode radiates. The larger the magnitude of λ_n, the more energy stored in the mode. The sign of λ_n indicates the type of energy storage associated with the mode. When λ_n is positive, the mode is inductive and when λ_n is negative, the mode is capacitive. When λ_n equals 0 the mode is resonant on the structure at that frequency. To better visualize λ_n, modal significance is defined by

$$MS = \left| \frac{1}{1 + j\lambda_n} \right|. \tag{1.9}$$

MS also reflects how well the mode radiates. As MS approaches 1, the mode radiates more energy and as MS approaches 0, the mode is storing more energy instead of radiating. Another important quantity for visualizing the modal structure is the characteristic angle, α_n which is defined as

$$\alpha_n = 180^\circ - \arctan\left(\lambda_n\right). \tag{1.10}$$

The characteristic angle is 180° when the mode is resonant, so that when a mode is radiating α_n is close to 180°. Characteristic mode theory allows modes to be found on the structure independent of the excitation. Because it is independent of the excitation, the theory allows the ground plane modes to be evaluated separately from the modes on the antenna element and the modes of the entire antenna structure.

1.2.3 Effect of Finite Ground Planes

Although much work has been done involving ESAs and characteristic mode theory, the effect of the finite ground plane is often left out of the discussion. Very often planar antennas are used in mobile applications because they are relatively inexpensive for their high performance. The antennas can also typically be created using the standard circuit board making processes and integrated into boards. One of the most common planar antennas is the PIFA. Because the PIFA is often mounted to a larger circuit board, much research has been done in order to optimize the design of PIFAs for specific applications. One of the main components varied in the PIFA is the size of the ground plane. At first researchers looked at the effect of changing ground plane size on bandwidth and discovered that the bandwidth is maximized

around .45λ [17]. Later, other researchers showed that ground plane size had significant effects on the radiation patterns and bandwidth [18]-[19].

While these studies examine the effects of the ground plane on bandwidth, they do not describe why the radiation patterns and bandwidth change so drastically and the size and shape of the ground plane is altered. Because mobile communications companies often use PIFAs, the ground plane studies have been completed; however, there are very minimal discussions about ground plane size and shape for ESAs. The studies in [17, 18, 19] all seem to indicate that the modal behavior of the ground plane might be able to account for the bandwidth fluctuations and the changes in radiation pattern.

It has already been shown that additional modes present on an antenna can allow for wider bandwidth than available from a single mode, but the author uses the entire structure to foster the dual mode operation [20]. Adams creates an antenna that has two modes with similar resonant frequencies. Because the bands from each mode overlap, the resulting bandwidth is larger than it would have been if only one mode was used. However, in this case the antenna element is still mounted to an infinite ground plane allowing for the approximation that the image currents appear on the opposite side. Much like the electrically small antenna research, this neglects the effect of the modes present on a finite ground plane. But, the research does give insight into what characteristics can be correlated with bandwidth maxima for structures. When two modes are resonant close together, a bandwidth maximum is created. If a ground plane structure can demonstrate the same behavior for certain lengths, the ground plane can create bandwidth maxima.

By understanding the modes present on the ground plane, it is possible to understand why bandwidth oscillations occur with size variations and explain the phenomenon seen by previous authors and antenna designers. This can also lead to further insight about how to utilize the existing structure and packaging to create better bandwidth than that achieved by the antenna on its own. Because of the size of the electronics, screen, and battery it is often necessary to have a ground plane that is substantially bigger than the space allotted to the antenna element. Taking advantage of the available structure will allow for a better antenna than when only optimizing the antenna element. With a better understanding of how these bandwidth maxima occur, it will be possible to extend the insight to other shapes of ground planes as well as to electrically small antenna elements.

1.3 Thesis Organization

In order to understand the how the finite ground plane affects the maximum attainable bandwidth for a structure, characteristic mode analysis will be applied to different antennas. This work focuses solely on changing the length of a rectangular ground plane in order to gain insight into antenna performance. The emphasis for this work is also on planar antennas and therefore much of the work will consist of an analysis of planar antennas.

Chapter 2 focuses on the effect of a lengthening ground plane on simple PIFAs with one feed and one short. It will detail the effects of the elongated ground plane on antenna performance. Next, the process for understanding the modes present only on the ground plane will be presented. Lastly, characteristic mode analysis will be performed on three different PIFAs to attempt to prove that the trends present on the first antenna are consistent for all PIFAs.

The next chapter extends the analysis technique described in Chapter 2 to ESAs developed by Van Niekerk. These antennas are still planar, but they are now electrically small. In the original work the antennas were evaluated using a large square ground plane. Characteristic mode theory will be applied to the ground plane for two different planar ESAs and analyzed to see if the same trends are present. The ESAs will then be built and measured to compare the simulated results to the measured results.

Chapter 4 will attempt to address the effect of copper thickness on electrically small antennas. The relationships between thickness, center frequency, and impedance are investigated for trends to help quantify the impact of finite conductivity and thickness on the antennas. This chapter will also try to quantify when it is appropriate to model metallic conductors as PEC to make simulation simpler. Lastly, Chapter 5 summarizes the completed work as well as ideas for future research.

CHAPTER 2

CHARACTERISTIC MODE ANALYSIS FOR THE GROUND PLANES OF PIFAS

2.1 Impact of the Ground Plane on PIFAs

This section focuses on the effect of the ground plane length on PIFAs with one feed and one short. The antennas will be analyzed and compared based on the bandwidth and radiation patterns. The first portion explains the design of the particular PIFA analyzed while the next section compares the simulated bandwidth to calculated bandwidth using equations given by Yaghjian and Best [21].

2.1.1 PIFA Design

The antenna designed to simulate the effects of ground plane size on bandwidth and radiation pattern is similar to the PIFA presented by Wu and Wong [17]. The dimensions were altered to shift the center frequency to 2 GHz arbitrarily. Figure 2.1 shows the top view of the antenna. Like Wu and Wong, the antenna is on a 6.4 mm air substrate.

To examine the effect of ground plane size in simulation, L was varied from the size of the element to about the size of a wavelength using HFSS®. As L increases, the size of the ground plane grows in the $+y$ direction only. The Smith chart in Figure 2.2 shows the S_{11} moving up and down the Smith chart while having the same basic shape as the ground plane size changes.

For the same lengths, L, the radiation patterns were also plotted and are shown in Figure 2.3. When the ground plane is small, the pattern is similar to that of a top-loaded monopole. When the ground plane is close to $\frac{\lambda}{2}$, the pattern begins to resemble that of a patch antenna. Here the ground plane is at a resonant length and begins to radiate more than the PIFA element. As the ground plane continues to get larger, the radiation pattern

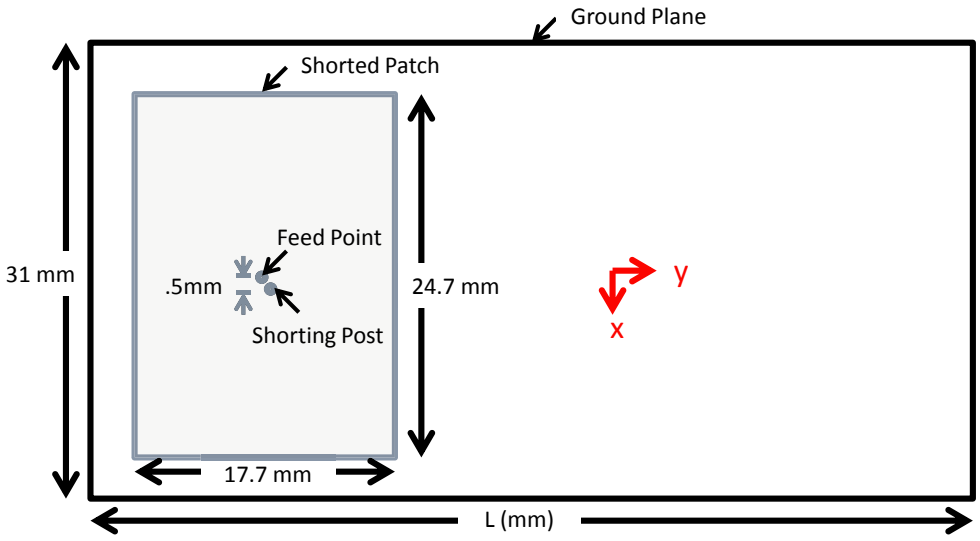

Figure 2.1: PIFA design

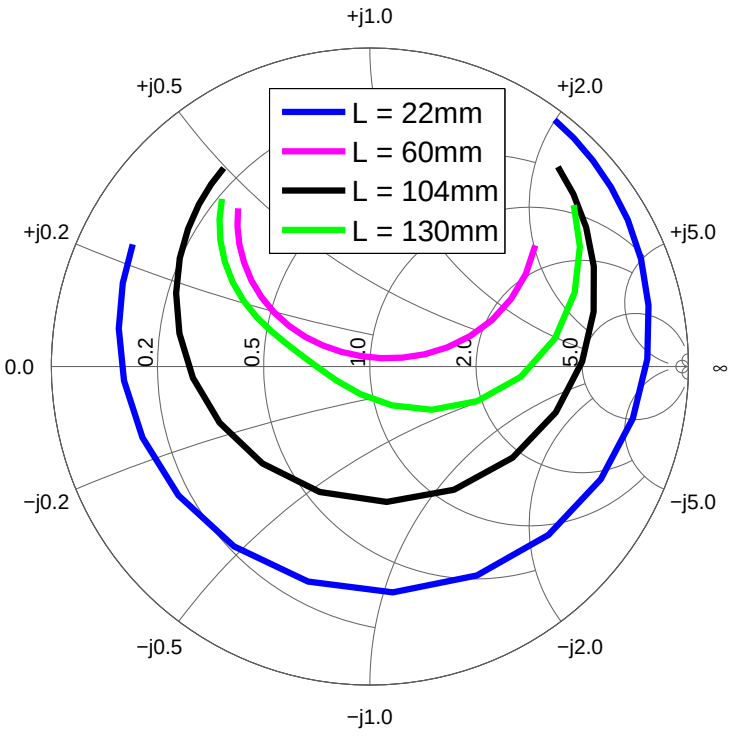

Figure 2.2: S_{11} for the PIFA antenna

becomes a combination of different traditional patterns. It also becomes more directive because the ground plane is significantly larger in the $+y$ direction. In both the $L = 104$ mm and the $L = 132$ mm radiation patterns, there are nulls in z and in y, showing the combination of the radiation patterns from both a monopole and a patch (similar to a combination of patterns from the structure with $L = 22$ mm and $L = 60$ mm).

2.1.2 Bandwidth

The last step is to examine the bandwidth achieved by the PIFA. Using the VSWR from the HFSS® simulated results, the 3:1 VSWR fractional bandwidth (FBW) is calculated. Although it is possible to examine each ground plane size and individually determine FBW, it is more desirable to calculate the FBW from the input impedance.

One way to convert from input impedance to FBW is presented by Yaghjian and Best [21]. They first convert input impedance to Q using

$$Q = \frac{\omega_0}{2R\left(\omega_0\right)}\sqrt{\left[R'\left(\omega_0\right)\right]^2 + \left[X'\left(\omega_0\right) + \frac{\left|X\left(\omega_0\right)\right|}{\omega_0}\right]^2}, \tag{2.1}$$

where $R(\omega_0)$ and $X(\omega_0)$ are the real and imaginary parts, respectively, of the input impedance of the antenna. Once there is a value for Q, the s:1 FBW of the antenna can be calculated using

$$FBW\left(\omega_0\right) = \frac{(s-1)}{Q\left(\omega_0\right)\sqrt{s}}. \tag{2.2}$$

Yaghjian and Best's work, however, assumes that the antenna is a singly resonant structure. As can be seen in Figure 2.2, this PIFA is not singly resonant so the equations are not strictly valid over the entire range of ground plane sizes. To compare the simulated and calculated values of the 3:1 VSWR bandwidth, both results are plotted together in Figure 2.4. At first the FBW using Equations 2.1 and 2.2 and the simulated 3:1 VSWR fractional bandwidth are very close until the first resonance of the structure. After the first resonance the two lines begin to diverge and continue to get farther apart as the ground plane gets larger. When the ground plan is small, the antenna acts more like a singly resonant structure as can be seen in the

radiation patterns from Figure 2.3. When $L = 22$ mm and $L = 60$ mm the patterns resemble those of singly resonant structures. As L gets larger, the patterns get more complicated, showing the presence of more than one mode, invalidating the assumptions for Equations 2.1 and 2.2. As the ground plane size increases, the bandwidth continues to oscillate although the magnitude of these oscillations get smaller.

As the ground plane gets larger, the radiation pattern changes significantly. The changing radiation patterns coupled with the 3:1 VSWR bandwidth indicate that there are multiple modes present on the structure. The existence of multiple modes causes the bandwidth to diverge significantly from previous equations to calculate bandwidth assuming that the antenna is a singly resonant structure. To account for this change, Section 2.2 performs a characteristic mode analysis on the antenna.

2.2 Characteristic Mode Analysis Applied to the Ground Plane of PIFAs

This section outlines a process using characteristic mode analysis to correlate the modes on the ground plane to bandwidth minima and maxima. First, section 2.2.1 describes the process and performs the analysis on the ground plane of a PIFA from the literature. Sections 2.2.2 and 2.2.3 perform the analysis on two other PIFA designs to validate the process. Section 2.2.2 addresses the impact of changing the PIFA's feed structure while Subsection 2.2.3 addresses the impact of shifting the center frequency and changing the size of the ground plane when the antenna is matched (matching point). The chapter closes with conclusions about the developed process.

2.2.1 Design Process

To understand the modal behavior of the PIFA, it is important to look at the modes on the finite ground plane while taking the height and feed structure of the antenna into account. To derive a process for determining the bandwidth of a PIFA based on only the finite ground plane and feed structure, the antenna in the previous section, shown again in Figure 2.5, is analyzed. In the figures showing the design of the antennas the x represents feed place-

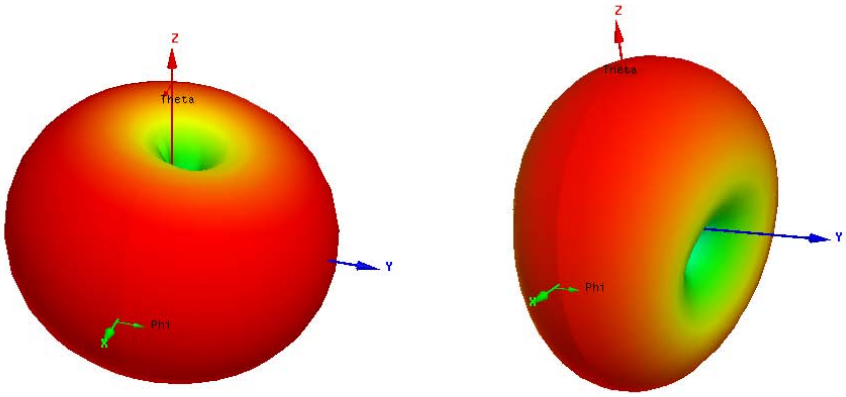

(a) L = 22 mm (b) L = 60 mm

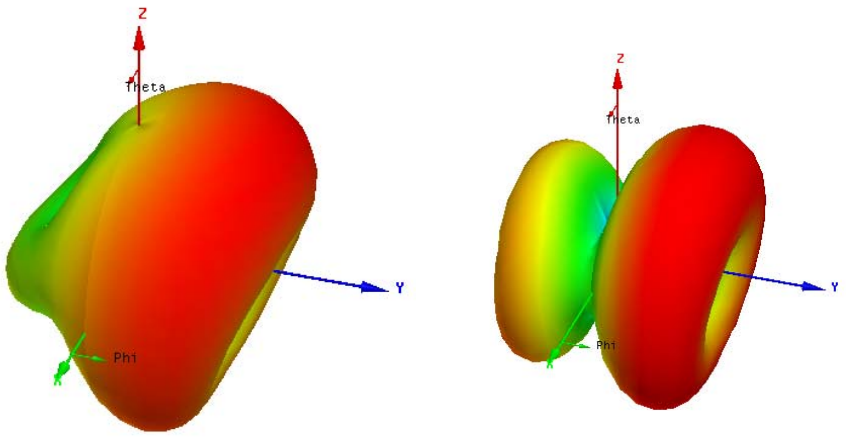

(c) L = 104 mm (d) L = 132 mm

Figure 2.3: Radiation patterns of the studied PIFA design for differently sized ground planes

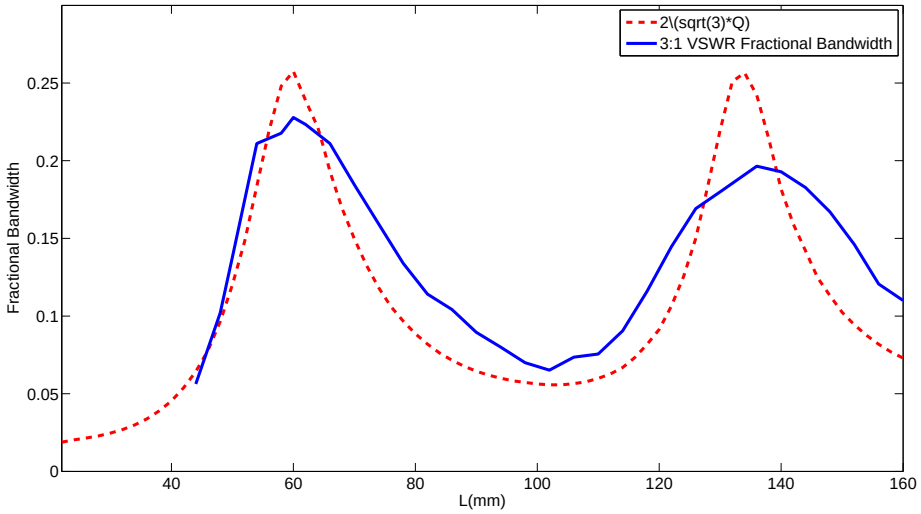

Figure 2.4: Fractional bandwidth comparison

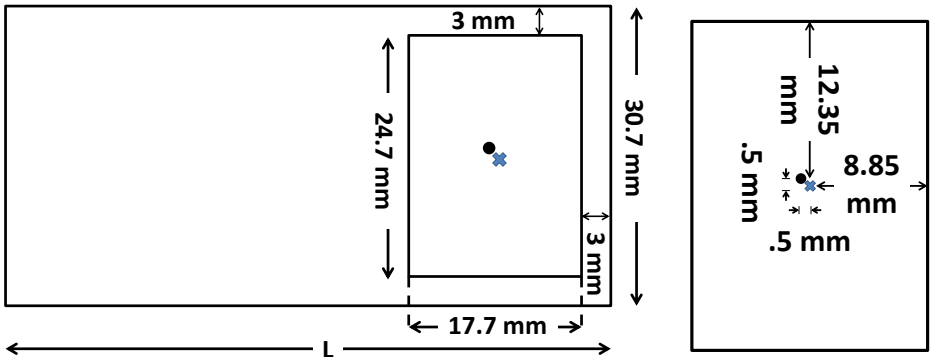

(a) PIFA Dimensions with Ground Plane (b) Zoomed Element

Figure 2.5: PIFA design and dimensions for antenna from previous work

ment and the • represents the short. The height of this and each subsequent antenna is 6 mm. When the distance between the PIFA element and ground plane is extremely small, it is extremely difficult to match the antenna to measure it on a 50Ω system with only one feed point and one short. For this reason, the height for all the antennas presented is greater than 0.04λ. For each antenna, the center frequency is determined by examining the bounds of the 3:1 VSWR bandwidth for each ground plane size. These center frequencies are averaged over all simulated ground plane sizes to determine the overall center frequency for the antenna. The changes in bandwidth over ground plane size are shown in Figure 2.6. Each PIFA design is first simulated in HFSS® to find the bandwidth minima and maxima. To better

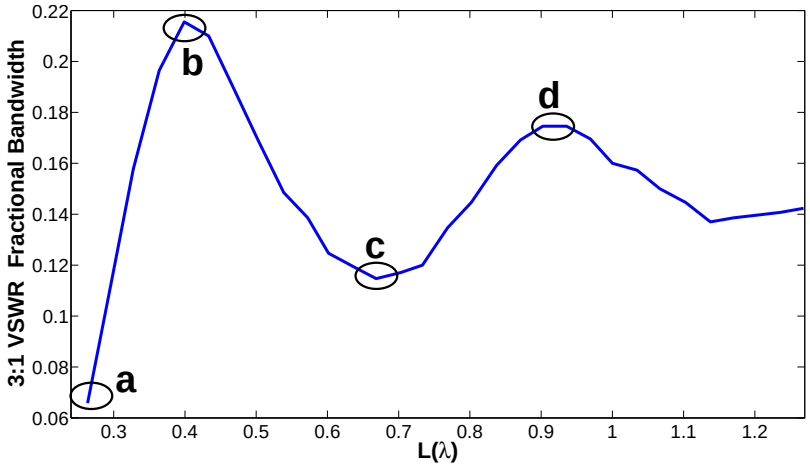

Figure 2.6: Change of 3:1 VSWR fractional bandwidth as the ground plane gets longer for PIFA shown in Figure 2.5

understand how the ground plane causes bandwidth fluctuations, the characteristic modes can be found when the finite ground plane is separated from the antenna element. However, only analyzing the ground plane neglects both the feed structure and the height of the antenna. To attempt to take the height and the feed structure into account, the element of the antenna is replaced by an infinite ground plane and then a characteristic mode analysis is performed. To perform the characteristic mode analysis, the antenna is simulated in FEKO® with the element replaced by an infinite ground plane. The simulated impedance matrix is then exported to MATLAB® to perform the rest of the characteristic mode analysis. At each point a, b, c, and d shown in Figure 2.6, the modal significance is evaluated when the ground plane and feed structure are situated over an infinite ground plane. Each of the modal significance plots in Figure 2.7 represent the modal significance of modes at a minimum or maximum bandwidth point from Figure 2.6. Figures 2.7(a) and 2.7(c) are representative of the modal significance at bandwidth minima. In both figures, there is one mode that is dominant and centered near the center frequency of the antenna. Figures 2.7(b) and 2.7(d) represent bandwidth maxima and the mode with the largest modal significance changes near the center frequency. Together the figures indicate that bandwidth minima correspond to the situation when one only mode is dominant on the structure near the center frequency and that bandwidth maxima correspond to when two modes are close together and the mode with

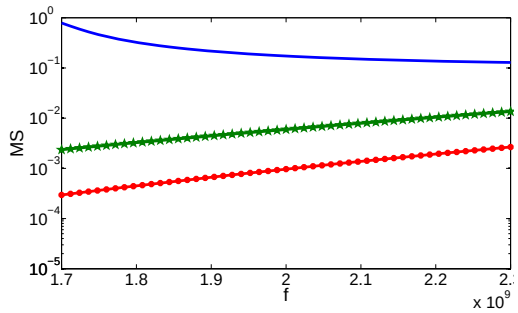

(a) L = 0.15λ

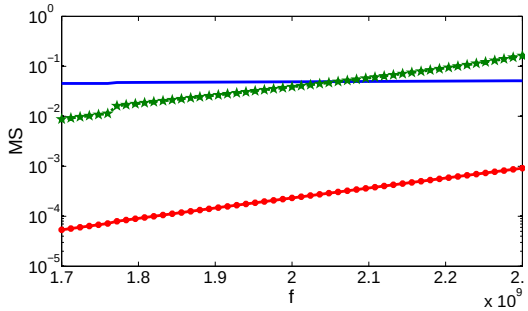

(b) L = 0.4λ

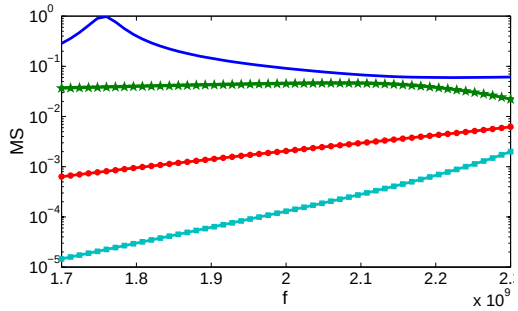

(c) L = 0.69λ

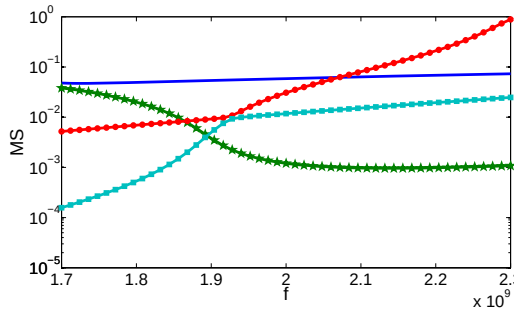

(d) L = 0.88λ

Figure 2.7: Depiction of the modal significance for differently sized ground planes. For each modal significance plot, the blue solid line represents the first mode and the green starred line represents the second mode. The red circle line represents the third mode and the fourth mode is represented by the cyan line with squares.

the maximum modal significance changes on or near center frequency of the antenna element attached to the finite ground plane.

2.2.2 Impact of Feed and Short Placement on Bandwidth Minima and Maxima

Second PIFA Design

A second antenna was designed to verify the relationship between bandwidth and modal significance. For the second antenna design, the element and height remain unchanged while only the feed structure was altered. The design for this second antenna can be seen in Figure 2.8 and the height of the antenna (not shown) is 6 mm. As seen in Figures 2.5 and 2.8, the feeding structure of the first antenna has both the feed and short near the center of the element while the second antenna has the feed and short toward the side of the element. The second antenna also has a significantly larger distance in between the feed and shorting pins, making it simpler to manufacture. Due to the change in feed, the center frequency for this antenna is slightly lower, at approximately 1.92 GHz.

Analysis

The 3:1 VSWR fractional bandwidth for this antenna is shown in Figure 2.9. The bandwidth minima and maxima for the second PIFA antenna design correspond to the same electrical lengths of the finite ground plane as in the first PIFA design. Because the feed structure and the frequency have shifted slightly, this provides further evidence that the ground plane and the modes on the ground plane are the main factor in understanding bandwidth oscillations. As before, the element is replaced with an infinite ground plane and characteristic mode analysis is performed on the structure. As seen in the analysis of the first antenna, bandwidth maxima correspond to places where two modes are close together and the mode with the highest modal significance changes near the center frequency of the antenna. Bandwidth minima correspond to where one mode has the highest modal significance and is resonant near the center frequency of the antenna. Both the first and second

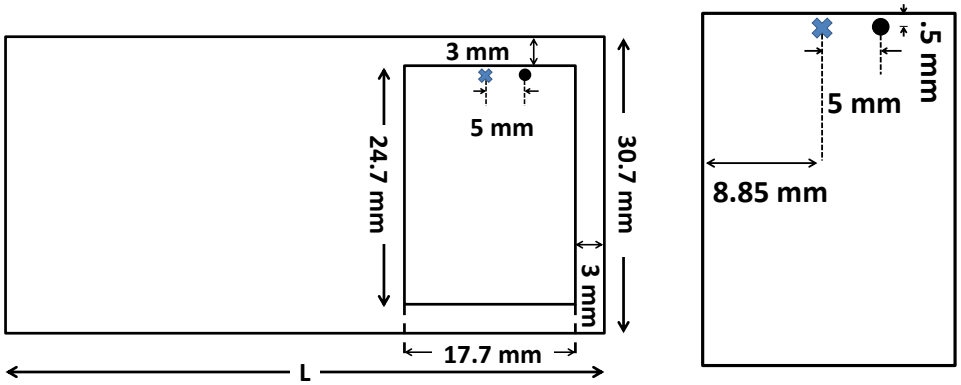

(a) PIFA Dimensions with Ground Plane (b) Zoomed Element

Figure 2.8: Second PIFA design with new feed and short positions

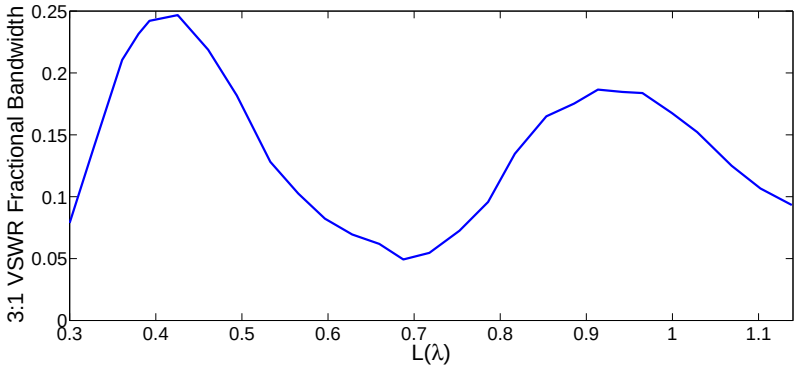

Figure 2.9: Change of 3:1 VSWR fractional bandwidth as the ground plane gets longer for PIFA shown in Figure 2.8

antenna designs demonstrate the same relationship between the bandwidth and modal significance. This leads to the conclusion that bandwidth maxima correspond to scenarios where two of the modes on the ground plane are close together and the mode with the highest modal significance changes near the center frequency regardless of the positions for the feed and shorting pins.

2.2.3 Impact of Center Frequency and Matching Point on Ground Plane Modes

Third PIFA Design

For both of the previously proposed antenna designs, the antennas were matched at one ground plane size and then L was varied to see the effect of the ground plane size on fractional bandwidth. The previous two antennas were matched at L = 0.4λ, which is very close to the maximum bandwidth point. To better understand the effect of the matching point on the bandwidth patterns, another new PIFA was designed. Instead of matching near a bandwidth maximum, this antenna was matched when L was 0.3λ. The geometry of the third antenna, shown in Figure 2.10, is slightly different to accommodate a different matching point and a slightly higher center frequency of 3.17 GHz. L was then varied from 0.2λ to 2.12λ to understand where bandwidth minima and maxima occurred for the third PIFA design. L was varied over a wider range to ensure that trends seen in the modal significance plots were preserved past the first two bandwidth minima and maxima. The 3:1 VSWR fractional bandwidth for this antenna is shown in Figure 2.11. The locations of bandwidth minima and maxima are similar to the minima and maxima seen in Figures 2.6 and 2.9. This further confirms the bandwidth minima and maxima have a strong relationship to the electrical size of the ground plane and are less reliant on the feed structure, element, matching point, and average center frequency of the antenna when the ground plane extends beyond the element.

Characteristic Modes and VSWR

For each minimum and maximum bandwidth point of the antenna, the modes, S parameters and VSWR were evaluated over the frequency band of interest. As with the previous two antennas, the element was replaced with an infinite ground plane and a characteristic mode analysis was performed on the structure for the values of L corresponding to bandwidth minima and maxima. The resulting modal significance plots showed the same behavior as the previous designs. Bandwidth maxima correspond to regions where two modes where close together and change modal significance on or near

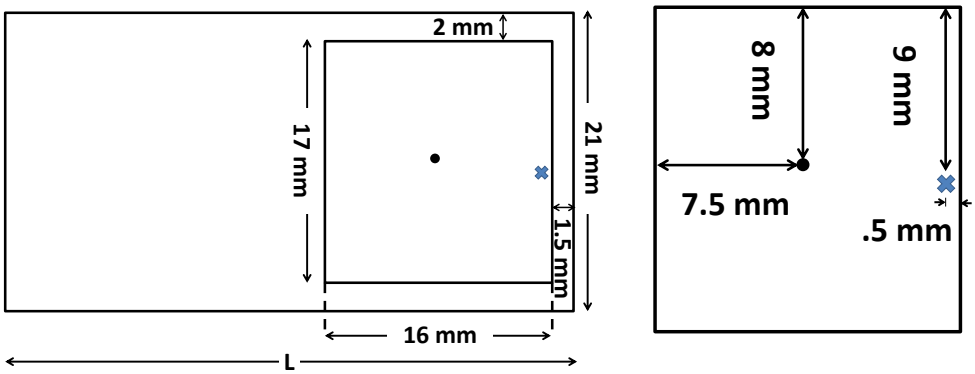

(a) PIFA Dimensions with Ground Plane (b) Zoomed Element

Figure 2.10: Third PIFA design for a higher center frequency

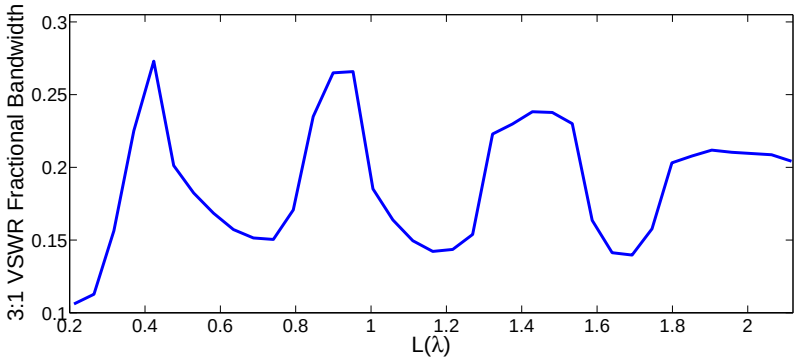

Figure 2.11: Change of 3:1 VSWR fractional bandwidth as the ground plane gets longer for PIFA shown in Figure 2.10

the center frequency and bandwidth minima occur where only one mode is dominant near the center frequency. Because L was varied over a larger range of electrical lengths, there were more bandwidth minima and maxima to investigate for this antenna. Even at bandwidth minima and maxima beyond $L = \lambda$, the same behavior was seen around the center frequency.

To understand how the modes affect the VSWR, Figure 2.12 shows the VSWR near bandwidth maxima and Figure 2.13 shows the VSWR near bandwidth minima. There are two dips in the 3:1 VSWR band that correspond to the two modes on the structure that switch modal significance near the center frequency. Because the modes are so close, they expand the bandwidth at these points. Comparatively, when the ground planes show only one dominant mode on the structure, the antenna has a smaller bandwidth and only one minimum point in the VSWR plot near the center frequency of the antenna as seen in Figure 2.13. The VSWR plots show how the modes are able to work together to make a larger bandwidth antenna compared to ground plane sizes that only support a single mode near the center frequency.

Three different PIFA designs were presented and the finite ground planes were evaluated using characteristic mode theory. Each PIFA design showed the same correlation between bandwidth maxima and minima with modal significance of the currents on the ground plane. This indicates that regardless of frequency, feed structure, or matching point, bandwidth maxima correspond to a change in the dominant radiating mode near the center frequency of the antenna and bandwidth minima correspond to one dominant mode over the band of interest. Other antennas were also simulated and follow similar trends to those presented in this paper. Because a multitude of PIFA antennas display the same properties, it follows that the trends are present for PIFA antennas with one feed and one shorting pin.

Because the process has been applied successfully to many different PIFAs, the next step is to apply it to other types of antennas. Although PIFAs are small antennas, they are not strictly electrically small. Planar antennas can also be made electrically small and thus the next chapter will investigate the effect of a finite ground plane on two different ESAs. Because the element for the ESA is so small, the ground plane will play a larger role in the bandwidth, radiation pattern, and gain of the structure. The next section details how the process can be applied to electrically small antennas.

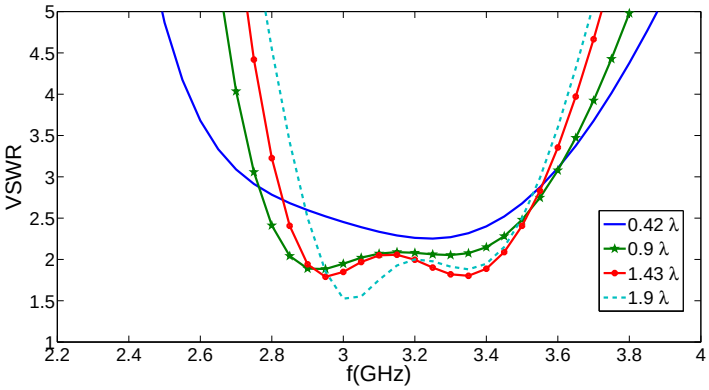

(a) VSWR

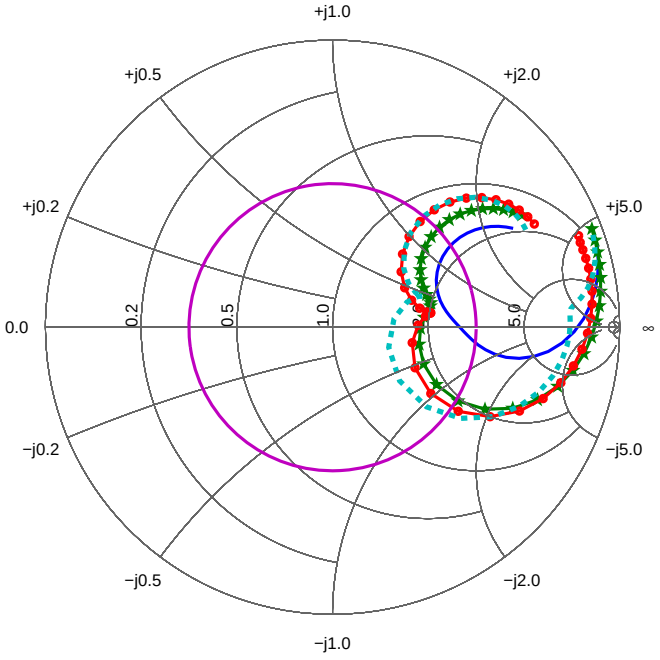

(b) Impedance from 2-4 GHz

Figure 2.12: Impedance and VSWR for maximum bandwidth points

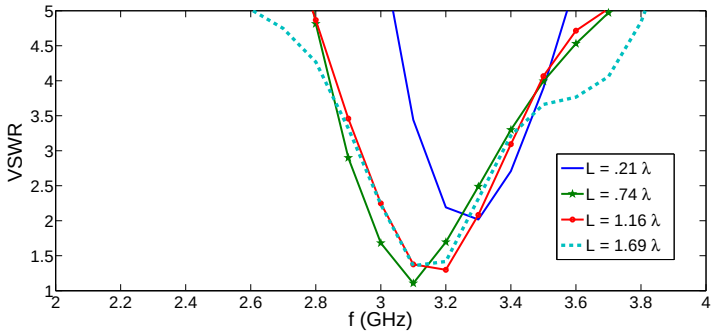

(a) VSWR

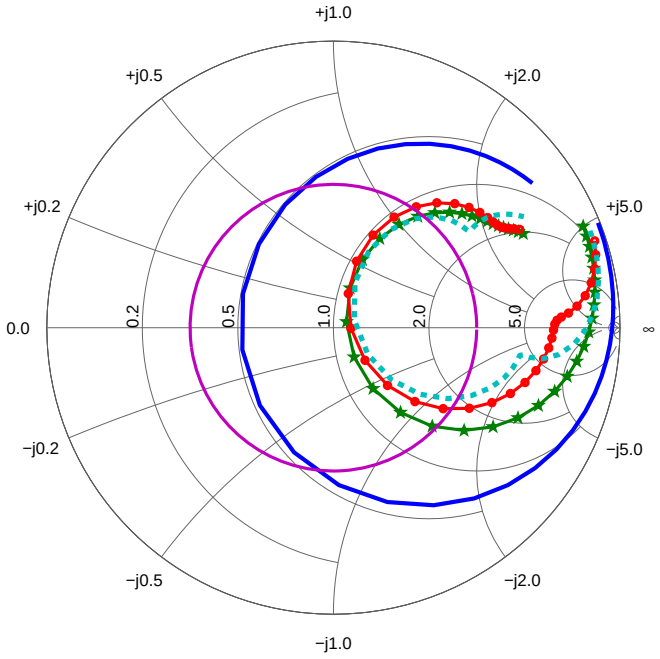

(b) Impedance from 2-4 GHz

Figure 2.13: Impedance and VSWR for minimum bandwidth points

CHAPTER 3

ELECTRICALLY SMALL ANTENNAS

3.1 Application of Developed Process

The previous chapter detailed a process for correlating bandwidth minima and maxima to ground plane length. This result, however, was only for the PIFA. The same process was applied to antennas designed by Van Niekerk [13]. The antennas are small cylindrical ESAs built on an air substrate. For the purposes of this project, only the horizontal and vertical feed elements were used. They are shown in Figure 3.1.

The large square ground plane from the original antennas is replaced with a rectangular ground plane. The ground plane has a fixed width in the x direction and grows in the $-y$ direction as shown in Figure 3.2, much like the ground planes for the PIFA antennas.

Just as before, the antennas were first simulated in HFSS® to find the bandwidth minima and maxima. Figure 3.3 shows how the bandwidth changes for both antennas as the ground plane gets longer.

As before, at each bandwidth minima and maxima, the circular element is replaced by an infinite ground plane and evaluated using FEKO. The modal significance for each minimum and maximum are shown in Figures 3.4 and 3.5.

Many of the pictures follow the same correlation that was seen in the previous section. Bandwidth maxima correspond to a plot where the mode with the highest modal significance changes near the center frequency of the antenna while bandwidth minima correspond to where the mode with highest modal significance is constant across the band. However, some of the maximum points do not have the same correlation. By making the ground plane slightly larger, however, the shifting modal significance does appear. Overall, because the characteristic mode simulations must use PEC, the center

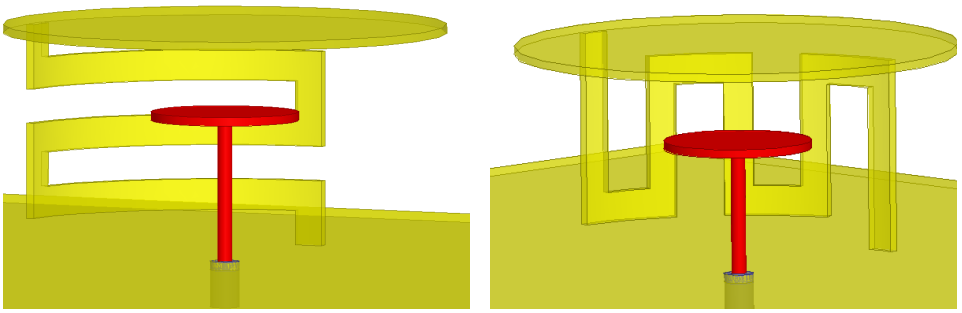

(a) Horizontal Element (b) Vertical Element

Figure 3.1: Electrically small antenna element designs, capacitive feed shown in red, from HFSS®

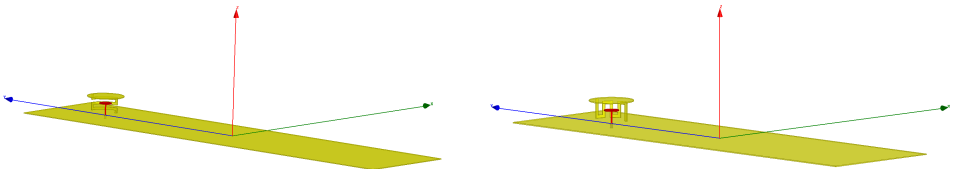

(a) Horizontal (b) Vertical

Figure 3.2: Electrically small antennas on rectangular ground planes

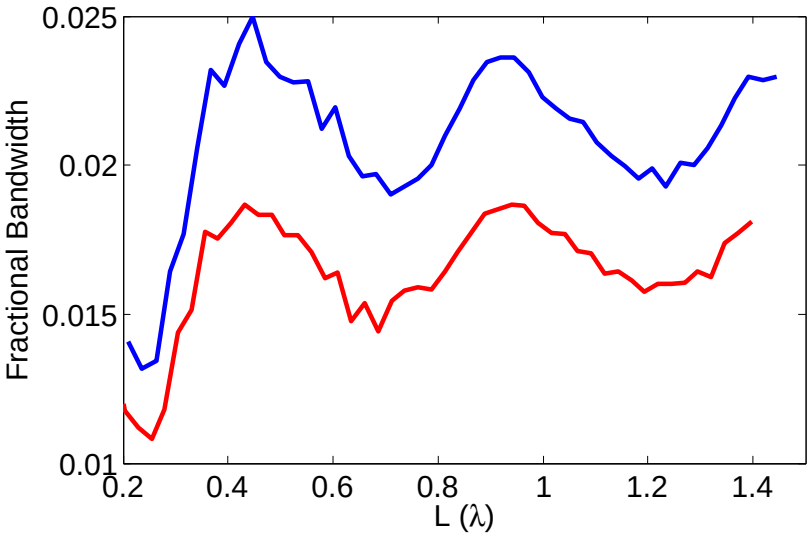

Figure 3.3: 3:1 VSWR fractional bandwidth for the horizontal and vertical ESAs as the rectangular ground plane gets longer

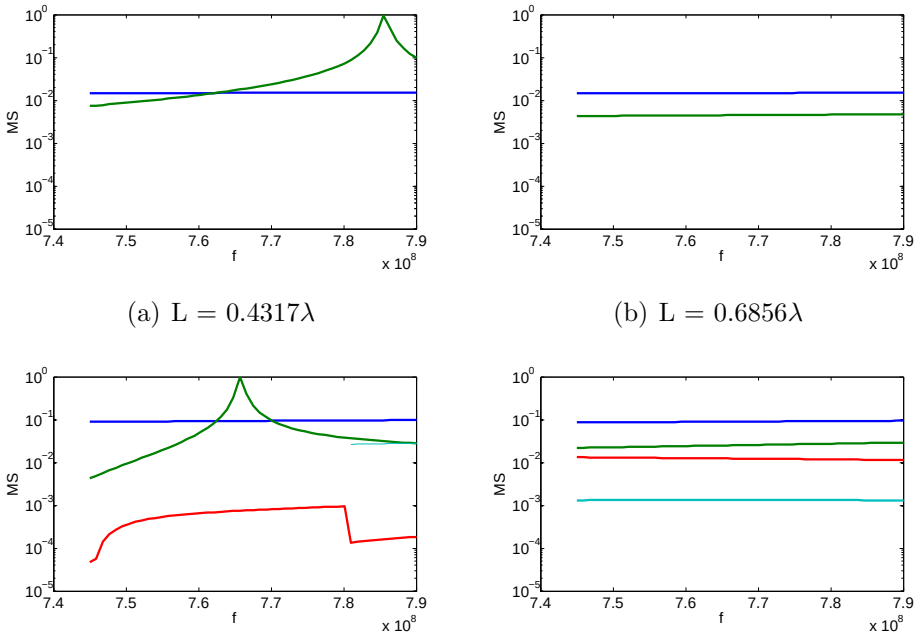

(a) L = 0.4317λ (b) L = 0.6856λ

(c) L = 0.9395λ (d) L = 1.1934λ

Figure 3.4: Depiction of the modal significance for differently sized ground planes with the vertical electrically small antenna. For each modal significance plot, the blue solid line represents the first mode and the green line represents the second mode. The red line represents the third mode and the fourth mode is represented by the cyan line.

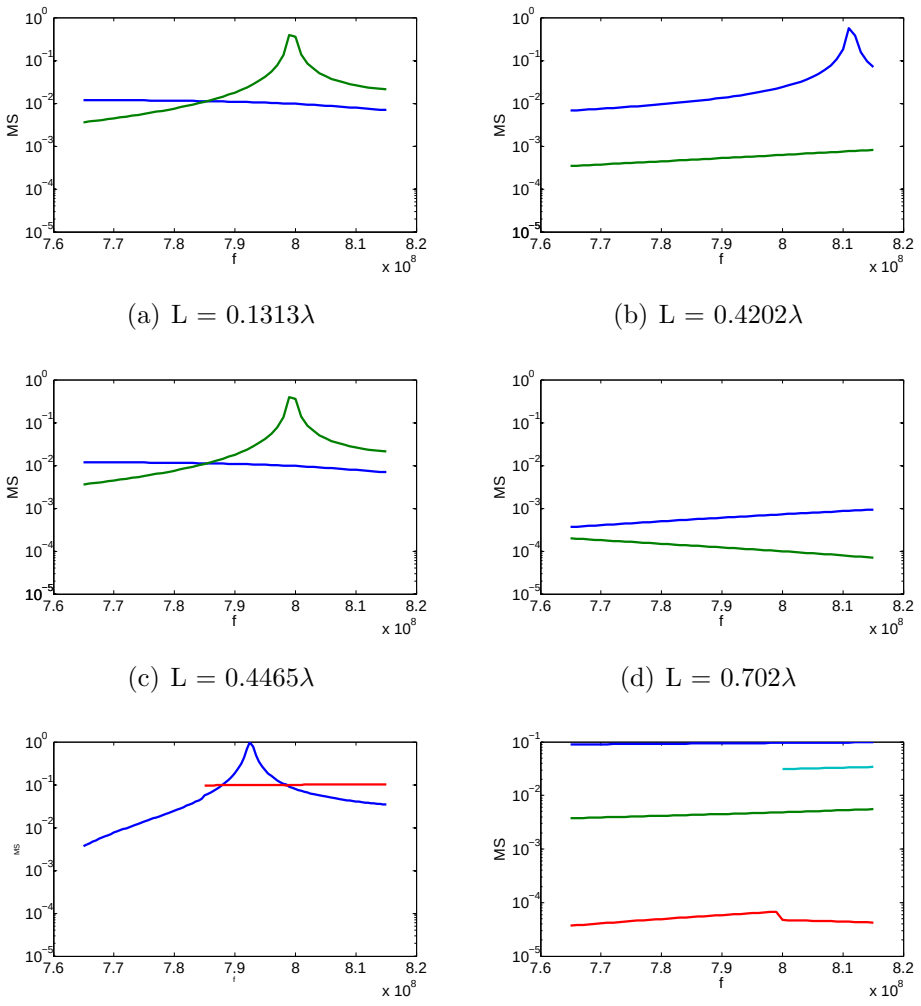

(a) L = 0.1313λ (b) L = 0.4202λ

(c) L = 0.4465λ (d) L = 0.702λ

(e) L = 0.9456λ (f) L = 1.235λ

Figure 3.5: Depiction of the modal significance for differently sized ground planes with the horizontal electrically small antennas. For each modal significance plot, the blue solid line represents the first mode and the green line represents the second mode. The red line represents the third mode and the fourth mode is represented by the cyan line.

frequency of the antenna using PEC is lower than the one using 0.0556 cm thick copper. Because the bandwidth for electrically small antennas is so small, the shift in center frequency between using PEC and thicker copper will cause the mode shift to occur at a larger physical size than predicted by the original simulations. Chapter 4 explains why in more detail.

3.2 Measurement of Electrically Small Antennas

To verify the simulated results are achievable, the antennas were built and measured. As discussed in previous sections, however, the antennas were not matched at all frequencies. This fact, coupled with the desire to study the effect of ground planes that are not infinite, makes it difficult to study the radiation pattern of the antennas. A balun must be used to try and keep the feed cable from being the dominant source of radiation. A balun was designed with a CMRR over 20 dB for the entire band from 750 MHz to 800 MHz. The balun, however, is typically a large piece of metal behind the antenna and thus was still greatly affecting the measured radiation pattern. The antennas were also then simulated with the balun attached in a variety of different orientations to better understand how the measured data compared to the simulated data. Because electrically small antennas are so sensitive, the patterns and bandwidth may not match entirely so it is important to simulate the antenna being measured as accurately as possible.

First, the bandwidths of the antennas were measured when the ground planes were at L = 0.25λ, 0.42λ, 0.7λ and, 0.94λ for each antenna. Overall the bandwidth was slightly larger than that predicted by the simulation and it is shown in Tables 3.1 and 3.2. However, this additional bandwidth is easily accounted for by extra loss in fabricating the antennas compared to the simulated values. There is more loss in the copper than simulated as well as in the SMA connector. The solder connections holding the small capacitive feed disk on could also be contributing to the loss in the antenna. The center frequencies of the simulated and measured antennas are also close together. The simulated horizontal antenna has an average center frequency of 788 MHz while the measured value is 785.8 MHz. The simulated vertical antenna has a simulated center frequency of 762 MHz while the measured is 757 MHz. If the measured values are normalized to the maximum value in

Table 3.1: Measured Bandwidth for Horizontal Electrically Small Antenna

Ground Plane Size (λ)	Bandwidth
0.24	0.0197
0.43	0.0372
0.71	0.0294
0.94	0.0365

Table 3.2: Measured Bandwidth for Vertical Electrically Small Antenna

Ground Plane Size (λ)	Bandwidth
0.25	0.0185
0.43	0.0327
0.68	0.0253
0.93	0.0318

simulation, the trends line up as seen in Figure 3.6.

The simulated and measured normalized radiation patterns are shown in Figures 3.7, 3.8, 3.9, and 3.10. In all figures, the solid blue line is the simulated data and the red dotted line is the measured data. The simulation and measured value are close but there are small differences. Some of the nulls are not as deep because of the small imperfections in the design of the antenna and slight differences between the simulated model and the built antenna. Also the antennas were fed using a string of baluns to minimize feed cable radiation. Unfortunately this also meant there was a large metallic structure behind the antenna. Although the situation was simulated as closely as possible, some of the measured values still do not match.

The measurements are very sensitive to slight changes in feed disk height, balun order, and cable placement. When the feed disk moves up and down, the center frequency and patterns change. Also, the feed cable still has some radiation even with the balun installed. This can cause the differences seen here. There is also more loss in the system than captured in the simulation. For this reason, the bandwidth is slightly larger than those predicted in simulation, but the same trends do occur. The two maximum points have larger relative bandwidths than the minimum points and the larger ground plane has a lower bandwidth than the small ground planes associated with a maximum. These measurements overall support the findings and use of the process.

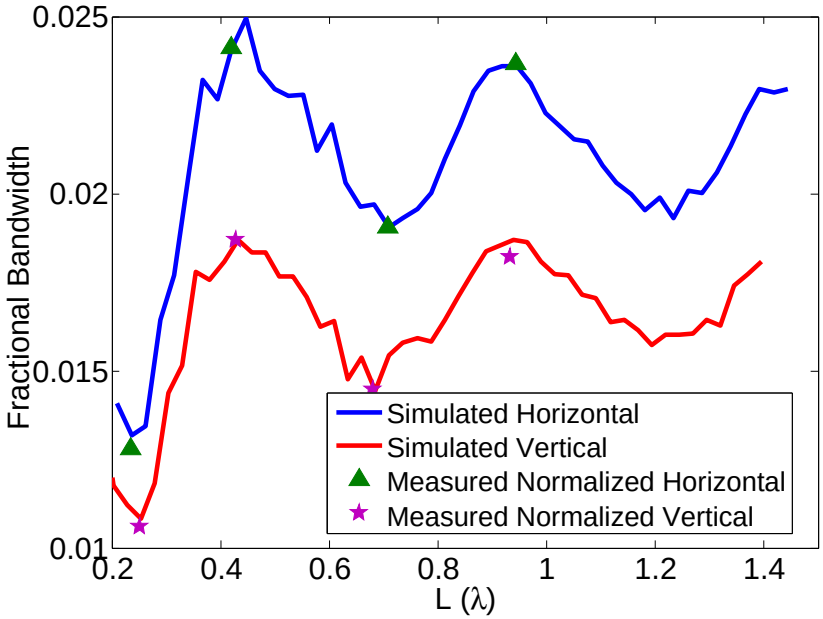

Figure 3.6: Comparison of simulated and measured data for the ESA bandwidth

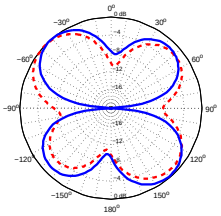

(a) L = 0.24λ Horizontal

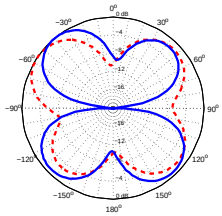

(b) L = 0.25λ Vertical

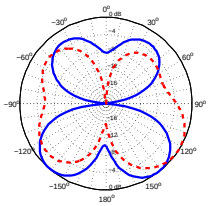

(c) L = 0.43λ Horizontal

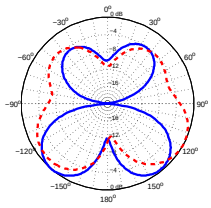

(d) L = 0.43λ Vertical

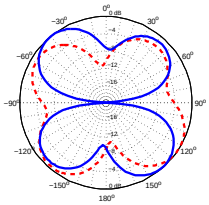

(e) L = 0.71λ Horizontal

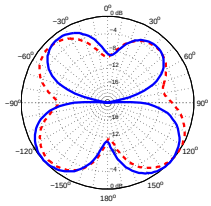

(f) L = 0.68λ Vertical

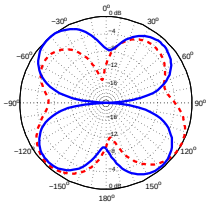

(g) L = 0.94λ Horizontal

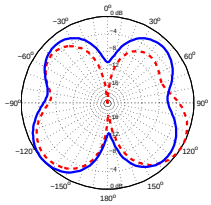

(h) L = 0.93λ Vertical

Figure 3.7: The normalized E_x polarizations for the XZ plane

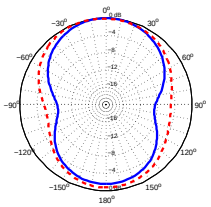

(a) L = 0.24λ Horizontal

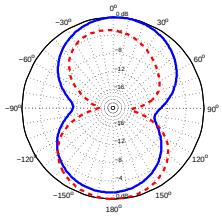

(b) L = 0.25λ Vertical

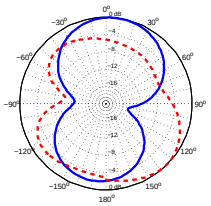

(c) L = 0.43λ Horizontal

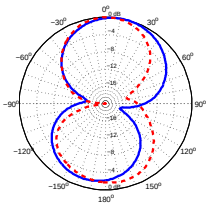

(d) L = 0.43λ Vertical

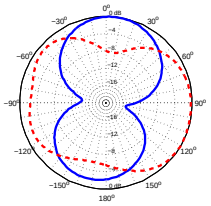

(e) L = 0.71λ Horizontal

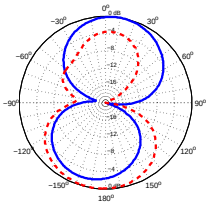

(f) L = 0.68λ Vertical

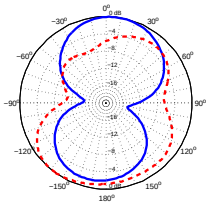

(g) L = 0.94λ Horizontal

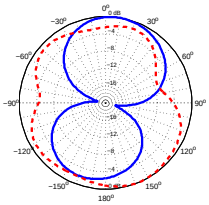

(h) L = 0.93λ Vertical

Figure 3.8: The normalized E_x polarizations for the YZ plane

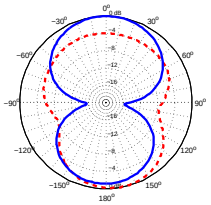

(a) L = 0.24λ Horizontal

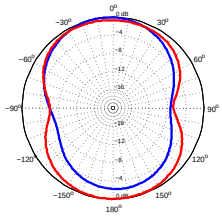

(b) L = 0.25λ Vertical

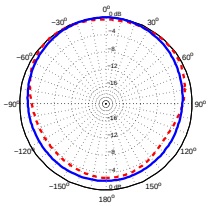

(c) L = 0.43λ Horizontal

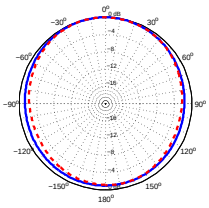

(d) L = 0.43λ Vertical

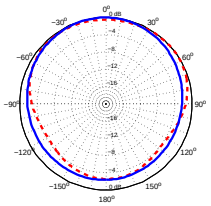

(e) L = 0.71λ Horizontal

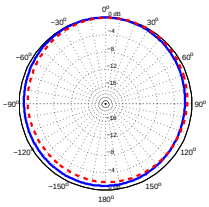

(f) L = 0.68λ Vertical

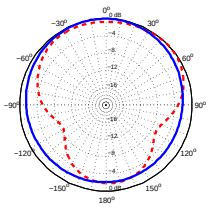

(g) L = 0.94λ Horizontal

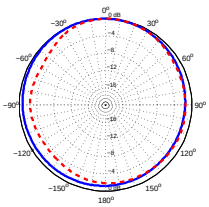

(h) L = 0.93λ Vertical

Figure 3.9: The normalized E_y polarizations for the XZ plane

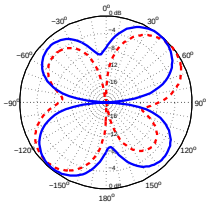

(a) L = 0.24λ Horizontal

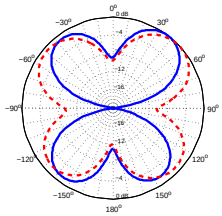

(b) L = 0.25λ Vertical

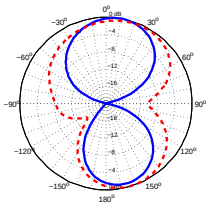

(c) L = 0.43λ Horizontal

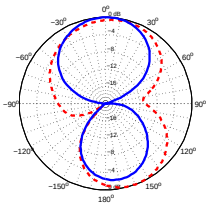

(d) L = 0.43λ Vertical

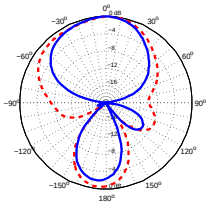

(e) L = 0.71λ Horizontal

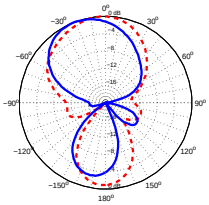

(f) L = 0.68λ Vertical

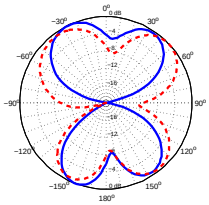

(g) L = 0.94λ Horizontal

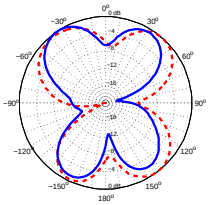

(h) L = 0.93λ Vertical

Figure 3.10: The normalized E_y polarizations for the YZ plane

CHAPTER 4

EFFECT OF COPPER THICKNESS

In the previous chapter, some of the crossing points for the modal significance did not appear exactly at the ground plane length corresponding to the bandwidth maximum. Although the crossing was at a ground plane length close to the maximum, the simulations did not match up as closely as they did for the PIFA antennas. The HFSS® simulation was done using 16 oz. copper while the characteristic mode simulations in FEKO® were done using PEC. The effect of the thickness of copper was studied to see if this difference could account for the slight differences in simulation results.

4.1 Using Previous Electrically Small Antenna Designs

Using the ESA designs from the previous section, the thickness of the copper was varied in HFSS® for the horizontal and vertical ESAs on a 16 cm length ground plane. Various copper thicknesses as well as PEC were evaluated to find the new frequency with the minimum VSWR. These designs, as in the previous chapters, were not matched. Figure 4.1 shows the change in center frequency as the copper gets thinner. The horizontal and vertical ESAs simulated with thick copper have a center frequency of 784.422 MHz and 761 MHz, respectively, while the corresponding PEC versions have a center frequency of 720.101 MHz and 716.625 MHz respectively. This large decrease is only due to the change in copper thickness. The center frequency of the antenna changes by 8.7% for the horizontal ESA and 6.2% for the vertical ESA. The slope for both ESAs in Figure 4.1 is linear; however, the curve corresponding to the horizontal ESA is steeper than that for the vertical ESA. This method does not allow changes in bandwidth or efficiency to be easily captured. Therefore each antenna will now be matched when the ground plane is 16 cm long. They will be compared for each thickness

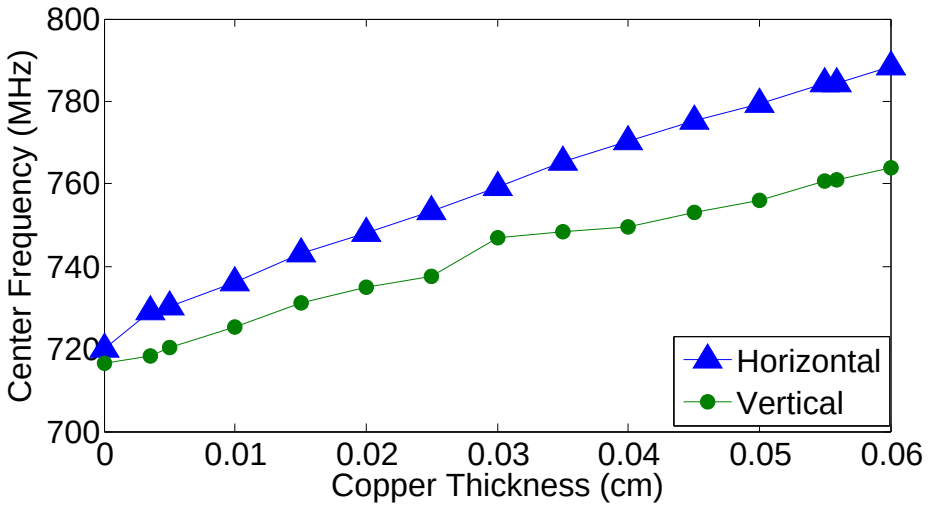

Figure 4.1: Change in center frequency as the copper thickness changed for the horizontal and vertical ESAs

of copper. The antennas are matched by slightly raising or lowering the capacitive feed disk for the antenna. This is the chosen method for matching the antennas because in the fabricated antennas, moving the feed disk up and down is an easy way to tune the antennas without fabricating the entire antenna over again.

4.2 Matched Electrically Small Antennas

Each antenna was matched for four different copper thicknesses and PEC. When the horizontal and vertical ESAs were matched the thicker copper corresponded to a center frequency of 769.4 and 745.5 MHz respectively which lowered to 705.779 and 693 MHz when the copper was replaced with PEC. The bandwidth was 2.859% and 2.414%, respectively, using thicker copper while it fell to 2.409% and 1.804% using PEC. The efficiency also fell as the copper got thinner, going from 94.31% to 93.77%, respectively, to 90.38% and 89.35% for the thinnest copper tested. The efficiency was 100% for the PEC, but that is expected. Figure 4.2 shows the change in center frequency, bandwidth, realized gain, and efficiency for the matched antennas. These plots are also relatively linear if the point for PEC is left off. Overall, center frequency, bandwidth, gain and efficiency increase with increased copper thickness.

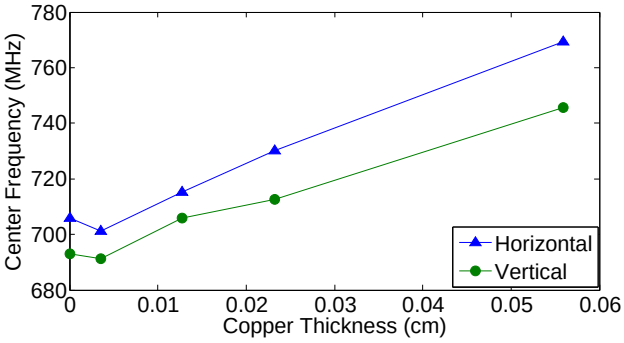

(a) Center Frequency

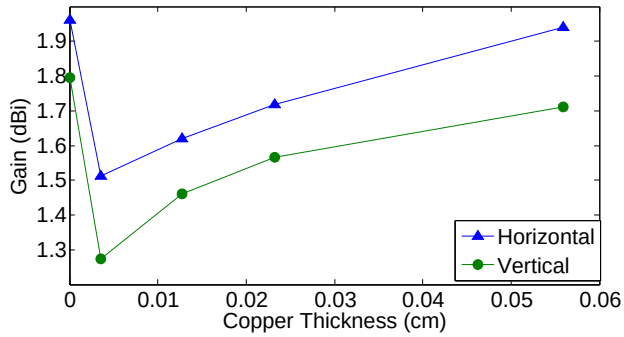

(b) Gain

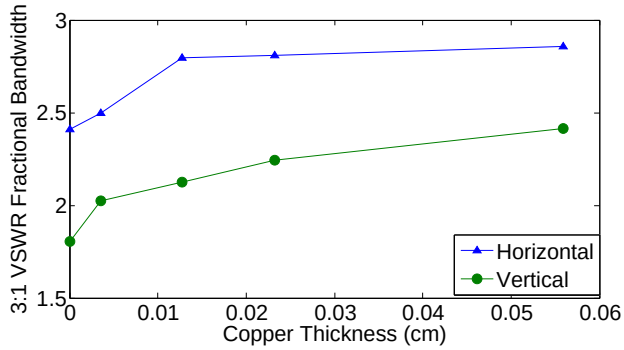

(c) Bandwidth

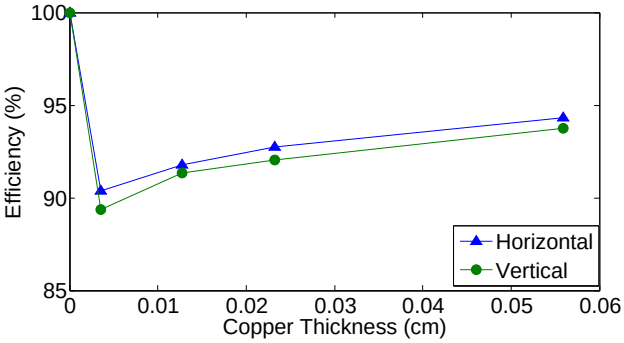

(d) Efficiency

Figure 4.2: Change in center frequency, gain, bandwidth, and efficiency for the ESAs as the copper thickness changes

Overall, the thickness of the copper has a significant effect on the center frequency, bandwidth, gain and efficiency of electrically small antennas. The change in center frequency for the PEC antenna makes λ_0 for the PEC simulation larger compared to λ from the simulation using copper. The PEC simulation puts 17 cm as approximately $0.42\lambda_0$ or 0.4465λ while the simulation using copper has 0.42λ at 16 cm as seen in Figure 3.5. This accounts for why the change was not seen at 0.42λ as predicted by the HFSS® simulations but was seen at 0.4465λ. The center frequency change is large enough to cause issues with the PEC and characteristic mode simulations. This problem did not arise with the PIFA antennas because the copper was thin enough that the center frequency was close to that given by the PEC approximation. Also, the bandwidths for the PIFAs are much larger overall so small changes in center frequency are less noticeable. However, with electrically small antennas, the bandwidth is between one and two percent. When the center frequency can change by six to eight percent, the bandwidth can shift away from the desired signal overall. To account for this the antennas should be simulated using both real conductors and PEC to understand the particular antenna's center frequency drift with copper thickness. Then the PEC results can be scaled up or down accordingly.

CHAPTER 5

CONCLUSIONS AND FUTURE WORK

5.1 Conclusion

In conclusion, characteristic mode theory can be used to analyze the effect finite ground planes. Examining just the ground plane and the feed structure, the placement of bandwidth minima and maxima can be predicted. Bandwidth maxima correspond to a portion where the mode that has the highest modal significance changes near the center frequency. Bandwidth minima occur where one mode has the highest modal significance across the entire frequency band.

The three different PIFA antennas presented here follow the model exactly. Each bandwidth minimum seen in HFSS® corresponds to one mode having the highest modal significance while each bandwidth maximum corresponds to two modes switching the mode with highest modal significance near the center frequency. The electrically small antennas follow the same trends when the thickness of the copper is taken into account. In Chapter 3, the maximum point did not line up directly with the transition. However, as seen in Chapter 4, the center frequency of the antenna is lower when modeling using PEC. Taking this into account, the bandwidth maxima and transitions line up appropriately. The electrically small antennas were also fabricated and measured. The measured results did not line up exactly with simulation because it is exceedingly difficult to make the antennas exactly as specified. Small changes in angle, height, and feed disk placement will alter the pattern and center frequency significantly. Also the fabricated antennas and measurement system has more loss compared to simulation, making the antenna have slightly larger bandwidth than predicted by simulation.

Chapter 4 details how the copper thickness affects the gain, bandwidth, center frequency, and efficiency results given by the simulation for the electri-

cally small antennas. The chapter also shows the linear relationships between these variables and allows for predictions to be made if the copper thickness for the antenna has to change. Overall the research confirms that the element has little effect on the bandwidth when the ground plane is larger than the element.

5.2 Future Work

In the future, this work can be extended to better understand where to place the feed points in order to create the two closely spaced modes needed for a bandwidth maximum to occur. By creating the separate modes at the appropriate frequency, this technique can be applied to scenarios where the size and shape of the ground plane are known. This would create a design process and make it easier to create new antenna designs instead of analyzing current antenna designs. This can also be applied to optimize antenna bandwidth in addition to understanding the ground plane size where the maximum will occur.

This work can also be extended to different shapes of ground planes. The work here focuses on rectangular ground planes, but the work can be applied to other shapes of ground planes. Differently shaped ground planes create different polarizations or radiation patterns allowing for more design parameters. These ground planes could also be compared to square and rectangular ground planes to better understand which shapes create the largest bandwidth when using smaller antenna elements.

Lastly, the characteristic mode theory code can be expanded to handle dielectric substrates. With this change in the available code, planar antennas that are on dielectric substrates can also be evaluated. Using air substrates neglects the effects of surface waves and other more complex phenomena. Most planar antennas, however, are fabricated using dielectric substrates so this extension would help with a larger variety of antenna designs.

REFERENCES

[1] H. Wheeler, "Fundamental limitations of small antennas," *Proceedings of the IRE*, vol. 35, no. 12, pp. 1479–1484, 1947.

[2] L. Chu, "Physical limitations of omni-directional antennas," *Journal of Applied Physics*, vol. 19, no. 12, pp. 1163–1175, 1948.

[3] R. Collin and S. Rothschild, "Evaluation of antenna Q," *IEEE Transactions on Antennas and Propagation*, vol. 12, no. 1, pp. 23–27, 1964.

[4] J. McLean, "A re-examination of the fundamental limits on the radiation Q of electrically small antennas," *IEEE Transactions on Antennas and Propagation*, vol. 44, no. 5, p. 672, 1996.

[5] H. Thal, "New radiation Q limits for spherical wire antennas," *IEEE Transactions on Antennas and Propagation*, vol. 54, no. 10, pp. 2757–2763, 2006.

[6] J. Adams and J. Bernhard, "A low Q electrically small spherical antenna," in *Proc. 2008 IEEE International Symposium on Antennas and Propagation*, 2008, pp. 1–4.

[7] S. Best, "A low Q electrically small magnetic (TE mode) dipole," *IEEE Antennas and Wireless Propagation Letters*, vol. 8, pp. 572–575, 2009.

[8] D. Sievenpiper, D. Dawson, M. Jacob, T. Kanar, S. Kim, J. Long, and R. Quarfoth, "Experimental validation of performance limits and design guidelines for small antennas," *IEEE Transactions on Antennas and Propagation*, vol. 60, no. 1, pp. 8–19, 2012.

[9] M. Gustafsson, C. Sohl, and G. Kristensson, "Physical limitations on antennas of arbitrary shape," *Proceedings of the Royal Society A: Mathematical, Physical and Engineering Science*, vol. 463, no. 2086, p. 2589, 2007.

[10] M. Gustafsson, C. Sohl, and G. Kristensson, "Illustrations of new physical bounds on linearly polarized antennas," *IEEE Transactions on Antennas and Propagation*, vol. 57, no. 5, pp. 1319–1327, 2009.

[11] A. Yaghjian and H. Stuart, "Lower bounds on the q of electrically small dipole antennas," *IEEE Transactions on Antennas and Propagation*, vol. 58, no. 10, pp. 3114–3121, 2010.

[12] G. A. Vandenbosch, "Simple procedure to derive lower bounds for radiation¡ formula formulatype=," *IEEE Transactions on Antennas and Propagation*, vol. 59, no. 6, pp. 2217–2225, 2011.

[13] C. Van Niekerk, "Analysis and design of compact low profile antennas for fixed volume applications," Ph.D. dissertation, Univ. of Illinois at Urbana-Champaign, Urbana,IL, January 2013. [Online]. Available: http://www.antennas.ece.illinois.edu

[14] R. Garbacz and R. Turpin, "A generalized expansion for radiated and scattered fields," *IEEE Transactions on Antennas and Propagation*, vol. 19, no. 3, pp. 348–358, 1971.

[15] R. Harrington and J. Mautz, "Theory of characteristic modes for conducting bodies," *IEEE Transactions on Antennas and Propagation*, vol. 19, no. 5, pp. 622–628, 1971.

[16] M. Cabedo-Fabres, E. Antonino-Daviu, A. Valero-Nogueira, and M. Bataller, "The theory of characteristic modes revisited: A contribution to the design of antennas for modern applications," *IEEE Antennas and Propagation Magazine*, vol. 49, no. 5, pp. 52–68, 2007.

[17] T. Wu and K. Wong, "On the impedance bandwidth of a planar inverted-f antenna for mobile handsets," *Microwave and Optical Technology Letters*, vol. 32, no. 4, pp. 249–251, 2002.

[18] A. Arkko, "Effect of ground plane size on the free-space performance of a mobile handset PIFA antenna," in *Proc. Antennas and Propagation Society Int. Symp.*, vol. 1. IET, 2003, pp. 316–319.

[19] M. Huynh and W. Stutzman, "Ground plane effects on planar inverted-f antenna (PIFA) performance," in *IEE Proc-H*, vol. 150, no. 4. IET, 2003, pp. 209–213.

[20] J. Adams and J. Bernhard, "A modal approach to tuning and bandwidth enhancement of an electrically small antenna," *IEEE Transactions on Antennas and Propagation*, vol. 59, no. 4, pp. 1085–1092, 2011.

[21] A. Yaghjian and S. Best, "Impedance, bandwidth, and Q of antennas," *IEEE Transactions on Antennas and Propagation*, vol. 53, no. 4, pp. 1298–1324, 2005.